the plant journal

SEB Society for Experimental Biology

The Plant Journal (2010) **62**, 135–147 doi: 10.1111/j.1365-313X.2009.04117.x

TECHNICAL ADVANCE

Automated tracking of stem cell lineages of Arabidopsis shoot apex using local graph matching

Min Liu[1], Ram Kishor Yadav[2], Amit Roy-Chowdhury[1,*] and G. Venugopala Reddy[2,*]

[1]*Department of Electrical Engineering, University of California, Riverside, CA, 92521 USA, and*

[2]*Department of Botany and Plant Sciences, and Center for Plant Cell Biology, University of California, Riverside, CA, 92521 USA*

Received 30 October 2009; accepted 3 December 2009; published online 1 February 2010.

[*]For correspondence Amit Roy-Chowdhury (fax 951 827 2425; e-mail amitrc@ee.ucr.edu) or G. Venugopala Reddy (fax 951 827 4437; e-mail venug@ucr.edu).

SUMMARY

Shoot apical meristems (SAMs) of higher plants harbor stem-cell niches. The cells of the stem-cell niche are organized into spatial domains of distinct function and cell behaviors. A coordinated interplay between cell growth dynamics and changes in gene expression is critical to ensure stem-cell homeostasis and organ differentiation. Exploring the causal relationships between cell growth patterns and gene expression dynamics requires quantitative methods to analyze cell behaviors from time-lapse imagery. Although technical breakthroughs in live-imaging methods have revealed spatio-temporal dynamics of SAM-cell growth patterns, robust computational methods for cell segmentation and automated tracking of cells have not been developed. Here we present a local graph matching-based method for automated-tracking of cells and cell divisions of SAMs of *Arabidopsis thaliana*. The cells of the SAM are tightly clustered in space which poses a unique challenge in computing spatio-temporal correspondences of cells. The local graph-matching principle efficiently exploits the geometric structure and topology of the relative positions of cells in obtaining spatio-temporal correspondences. The tracker integrates information across multiple slices in which a cell may be properly imaged, thus providing robustness to cell tracking in noisy live-imaging datasets. By relying on the local geometry and topology, the method is able to track cells in areas of high curvature such as regions of primordial outgrowth. The cell tracker not only computes the correspondences of cells across spatio-temporal scale, but it also detects cell division events, and identifies daughter cells upon divisions, thus allowing automated estimation of cell lineages from images captured over a period of 72 h. The method presented here should enable quantitative analysis of cell growth patterns and thus facilitating the development of *in silico* models for SAM growth.

Keywords: shoot apical meristem, stem-cells, cell tracking, cell segmentation, image registration.

INTRODUCTION

A local spatio-temporal coordination of cell growth and cell division plays a critical role in morphogenesis of both the plant and the animal tissues. The subject of this study, the shoot apical meristems (SAMs) also referred to as the stem-cell niche, is the most important part of the plant body plan because it supplies cells for all the above ground plant parts such as leaves, branches and stem. Despite a continuous displacement and diversion of cells into a differentiation program, the size of stem-cell niche remains relatively constant. Therefore, a tight spatio-temporal coordination between stem-cell division dynamics and rates of differentiation of stem-cell progeny is critical to maintain a stable SAM. However, the causal link between cell growth and cell division and how they, in turn, affect organ formation is not well understood. This is mainly due to a lack of quantitative understanding of cell growth patterns. Therefore, the development of computational platforms that are capable of identification of cellular coordinates, automated tracking of cells and cell division events from fluorescent 4-D (3-D image stack + time) images acquired by using laser

scanning confocal microscopy is important. Such computational platforms would facilitate the quantification of cellular parameters such as rates and patterns of cell expansion, orientation and rates of cell division, and extraction of such information may lead to the development of growth models that can explain the causal relationships between cell deformation dynamics, cell growth and cell division patterns. This process is a computational challenge that has universal application to all developmental fields, both animals and plants. In this work, we present a method to automatically register cell positions, and compute cell lineages (i.e. cell tracks through cell divisions) from the 4-D image stacks of SAMs.

SAMs of model plant *Arabidopsis thaliana* consist of approximately 500 cells (at inflorescence stages) and they are organized into distinct spatial domains as well as multiple cell layers that are clonally distinct from each other. The central zone (CZ) of the SAM harbours a set of stem-cells that divide at a relatively slower rate. The progeny of stem-cells enter the flanking peripheral zone (PZ) and also the Rib-meristem (RM) which is located beneath the CZ where they differentiate (Meyerowitz, 1997). Apart from this radial organization, the SAM of *Arabidopsis* is a multilayered-structure, organized into three clonally distinct layers of cells (Figure 1). The cells in the outermost L1 layer and the sub-epidermal L2 layer divide in anticlinal orientation (perpendicular to the SAM surface), while the underlying corpus forms a multi-layered structure where cells divide in random planes. Thus, the SAM stem-cell niche represents a dynamic and interacting network of functionally distinct cell types, exhibiting coordination between cell division dynamics and displacement of the progeny cells, both within and across clonally distinct layers (Meyerowitz, 1997). Regulated patterns of cell division is critical to ensure SAM function because other mechanisms of tissue homeostasis such as cell migration and cell death are not detected during SAM development. Earlier genetic studies have revealed that the cellular identities, their functions and growth patterns are regulated by diverse positional and environmental signals. The challenge for the future is to understand how diverse signals impinge on varieties of cellular behaviors such as cell division rates and cell expansion patterns to ensure tissue homeostasis in SAMs.

Our current knowledge of cell division patterns is derived from earlier studies carried out on several different plant species by employing varieties of analytical methods (Steeves and Sussex, 1989; Meyerowitz, 1997; Lyndon, 1998). Cytological studies and analysis of distribution of mitotic cells have revealed that the CZ cells divide more infrequently than cells in the PZ. The serial replica method has been employed to generate developmental time series of SAM surface and these studies have produced quantitative description of cell expansion behavior and associated changes in SAM shape (Hernandez *et al.*, 1991; Dumais and Kwiatkowska, 2002; Kwiatkowska and Dumais, 2003; Kwiatkowska, 2004). A careful and comprehensive morphometric analysis involving counting of mitotic figures from a large number of SAMs in *Arabidopsis thaliana* has yielded a composite view of mitotic activity (Laufs *et al.*, 1998). The development of live-imaging methods and suitable fluorescent markers has facilitated continuous visualization of given SAMs for several days (Grandjean *et al.*, 2004; Reddy *et al.*, 2004). Though these studies have yielded a dynamic description of mitotic activity, these data sets are under-utilized in obtaining quantitative measurements of cell behaviors. Therefore it is necessary to develop new computational tools for automatic detection and tracking of cells for extracting the cellular positions of all cells of SAMs from time-lapse datasets. In this study we report the development of cell tracking algorithm which has been implemented on SAM cells of *Arabidopsis thaliana.*

We have used confocal laser scanning microscopy to observe given set of Sams labeled with plasma membrane-localized yellow fluorescent protein (YFP), repeatedly for about 3 days by taking serial images at every 3-h intervals (Figure 1). The images obtained from live-imaging study can be noisy due to the poor signal to noise ratio; thus, the tracking method has to be robust enough to account for this noise. This apart, the cells are highly clustered together in space which presents a significant challenge in maintaining the correspondences of individual cells over extended periods of time.

One of the well known approaches in tracking cells is based on level-sets. A level-set is a collection of points over which a function takes on a constant value. The multiple-level-set approach is an active-contour based algorithm, which simultaneously segment cells and also tracks them (Li and Kanade, 2007). In this case, every cell is represented by a separate level-set function, wherein every level set function behaves like an active contour which gradually evolves toward the boundary of cells Therefore it has been adopted for obtaining cell segmentation (Chan and Vese, 2001). However, the level set method is not suitable for tracking of SAM cells because of several reasons. First, the cells are in close contact with each other. Second, the SAM cells share similar features with respect to their shapes and sizes. Third, large parts of images may be noisy at a particular time instant due to a low signal to noise ratio.

Given sets of segmented cells from the time lapse imagery, tracking of cells over time is essentially a point matching problem. One of the most popular solutions to point matching problem has been the Softassign Procrustes algorithm, which has been applied to compute cell lineages, and it has been improved further to detect cell divisions (Chui, 2000; Gor *et al.*, 2005; Rangarajan *et al.*, 2005). The Softassign method uses the information on point location to simultaneously solve both the problem of global correspon-

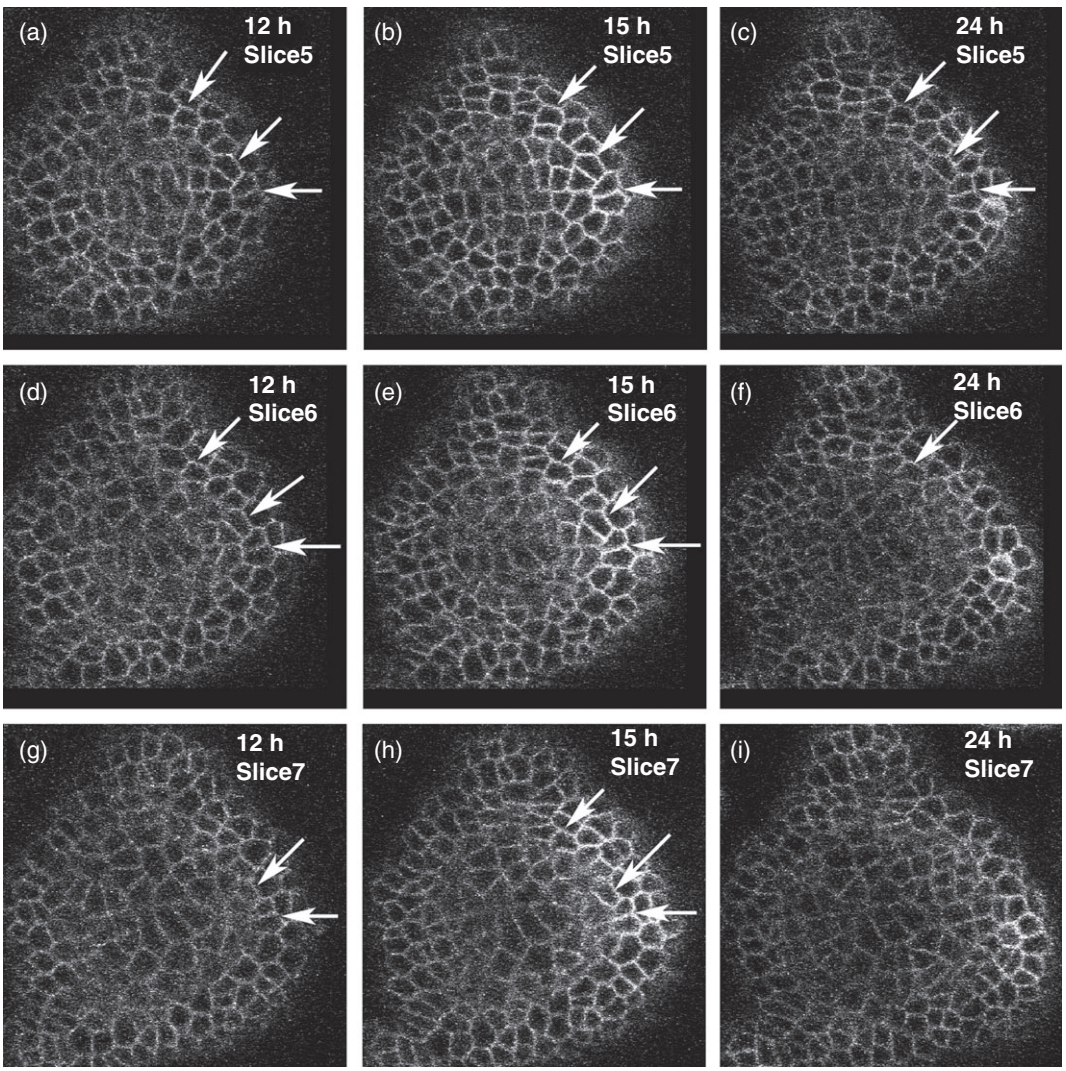

Figure 1. Time-lapse imagery of SAMs labeled with plasma membrane localized YFP.
Examples of three image slices (vertical columns) at three time instants (horizontal column).
(a–c) Arrow show same set of cells at time points noted on each panel. Cross-sectional images of SAMs depicted in the vertical columns are separated by 1.5 μm, while the size of a single cell is about 5 μm in diameter. Therefore each cell is represented in two or three consecutive slices.
(a, d, g) Arrows correspond to the optical sections of same cells located in different depths.
(a–c) Belong to slice 5; (d–f) belong to slice 6; and (g–i) belong to slice 7. Note the representation of several cells in three consecutive sections (arrows). The fusion of tracking outputs from three consecutive slices will account for cells that may not be imaged properly in one of the slices and also accounts for manual errors of imaging that contribute to misrepresentation of same cells in different optical slices across time points.

dence as well as the problem of affine transformation between two time instants iteratively. Although this method can be applied in aligning global features, it can produce errors in finding the local correspondences of individual cells. Therefore, calculation of local neighborhood structures of cells is crucial in tracking cells of similar shapes that lie in close proximity as in the case of SAMs (Figure 1). In the proposed approach, we consider information about the geometrical and topological inter-relationships between local neighborhood structures of cells that exist in clusters/groups, and this approach is expected to improve the stability of tracks, especially in the case of noisy time lapse images and also the anticipated errors in segmentation process (Zheng and Doermann, 2006).

In this paper, we present a heuristic graph matching method, wherein the matching problem is solved in a progressive manner (i.e. cell by cell), by obtaining correspondences from local graphs generated at different time instants (Gold and Rangarajan, 1996; Fazl-Ersi *et al.*, 2007). We have exploited the local geometrical and topological features of cells to generate graphs of the local neighborhood of each cell (Figure 3a,b). This process is followed by matching of the relative positional information of cells, such as the length and orientation of the edges with

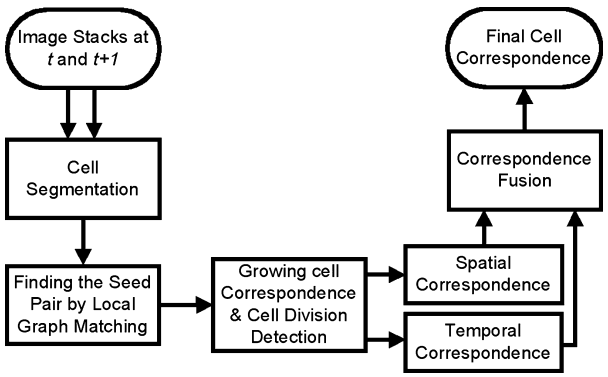

Figure 2. Diagrammatic representation of local graph-matching and spatio-temporal fusion based cell tracking for image stacks taken at two consecutive time points.
The level set segmentation will provide information on cellular parameters such as the centroids of cells, their area, and orientation of cell division to the tracker. This information is essential to find the seed cell pair by local graph matching method. Starting from this seed pair, we grow correspondences among neighboring cells by computing the similarity of local regions in the graph, and at the same time detect cell divisions by examining changes in the topology of the graph. This method allows us to compute correspondences of given cells both across slices taken at a give time point (spatial correspondence) and also across different time instants (temporal correspondence). The fusion of tracking output from both the temporal correspondence and spatial correspondence resulted in improved tracking efficiency.

respect to their nearest neighbors to find the most similar local graph pair between two time instants. This process provides a *seed* (initial) cell pair and the seed pair is used as a starting point to calculate similarities between local regions in the graph by progressively moving outwards (from this seed pair) to obtain correspondences of neighboring cells (Reuille *et al.*, 2005). This process is continued recursively to find correspondences of all cells (see Figure 3). We demonstrate that the method presented here has greater robustness over the global matching methods (Gor *et al.*, 2005), especially in cases where the images are noisy and which in turn results in poor segmentation. We have also used integration or fusion of tracking results over the entire four-dimensional (4D) image stack to improve the tracking efficiency, unlike earlier methods which have employed tracking on single-layer of cells or 3D-reconstructed surface-layer (Gor *et al.*, 2005; Reuille *et al.*, 2005). As every cell in the image stack is usually represented in three consecutive optical slices obtained along Z-dimension, it provides an opportunity to track the same cell thrice. We show that the integration or fusion of tracks from three consecutive slices greatly improves the tracking efficiency by accounting for cells that were not properly segmented in one of the three slices due to poor image quality. We have also applied the fusion idea in the cell lineage computation process, wherein we have integrated the cell lineages computed along different paths to track most of the cells in the entire L1 layer over a substantial period of time.

RESULTS

Collection of time-lapse imagery of actively developing SAMs

We have used plasma membrane-localized Yellow fluorescent protein (YFP), 35S::YFP29–1 expressed over ubiquitous promoter to visualize cell outlines or boundaries of all cells to follow cell division and expansion patterns (Figure 1) (Cutler *et al.*, 2000; Reddy *et al.*, 2004). We have used confocal laser scanning microscopy-based live-imaging set up to acquire a series of time-lapse images of 4-D stacks. Each 3-D stack was taken at every 3 h and it consists of a series of images of optical cross-sections of SAMs that are separated by approximately 1.5 μm. The sectioning of individual cells of 5 μm into 1.5 μm thick slices resulted in a given cell being represented in three consecutive slices (Figure 1). We have used all three sections of a given cell, at a given time point, for tracking purposes. Obtaining correspondence of a given cell across slices is referred to as spatial correspondence and obtaining correspondence of cells across time instances is referred to as temporal correspondence (Figure 2). For experiments described in this paper, we have used a 4D image stack of SAMs observed along 24 consecutive time instants, with the time interval of 3 h between two consecutive instants. The image stacks were registered prior to the tracking by using the alignment method of maximization of mutual information (Viola and Wells, 1995; Maes *et al.*, 1997). Image registration was applied to obtain global alignment of the images and it is achieved by optimizing a matching criterion between images (i.e. the mutual information).

From cells to graphs

As an initial step, we segmented SAM cells that are labeled with plasma membrane-localized YFP by employing existing level set segmentation methods (Figure 3a–h) (Chan and Vese, 2001). Upon obtaining a collection of segmented cells from time-lapse imagery, we created a graphical abstraction of segmented cells. This process involved representing every cell by a vertex and connecting neighboring vertices by an edge (Figure 3a,b). The Delaunay neighbors of cell c (i.e. the ones that share an edge of the Delaunay triangles with cell c) were considered as its neighboring cells and they were denoted by the neighborhood cell set $N(c)$ (Figure 3a,b). The structure of these graphs automatically includes the relative positional information of cells, such as the distance between two neighboring cells (the edge length) and the edge orientation. The topology and the geometry of the local graphs are not expected to change dramatically between two consecutive time instants separated by approximately 3 h unless the cells divide or the images are noisy. With these conditions satisfied, the corresponding cells across time were identified by matching the respective local

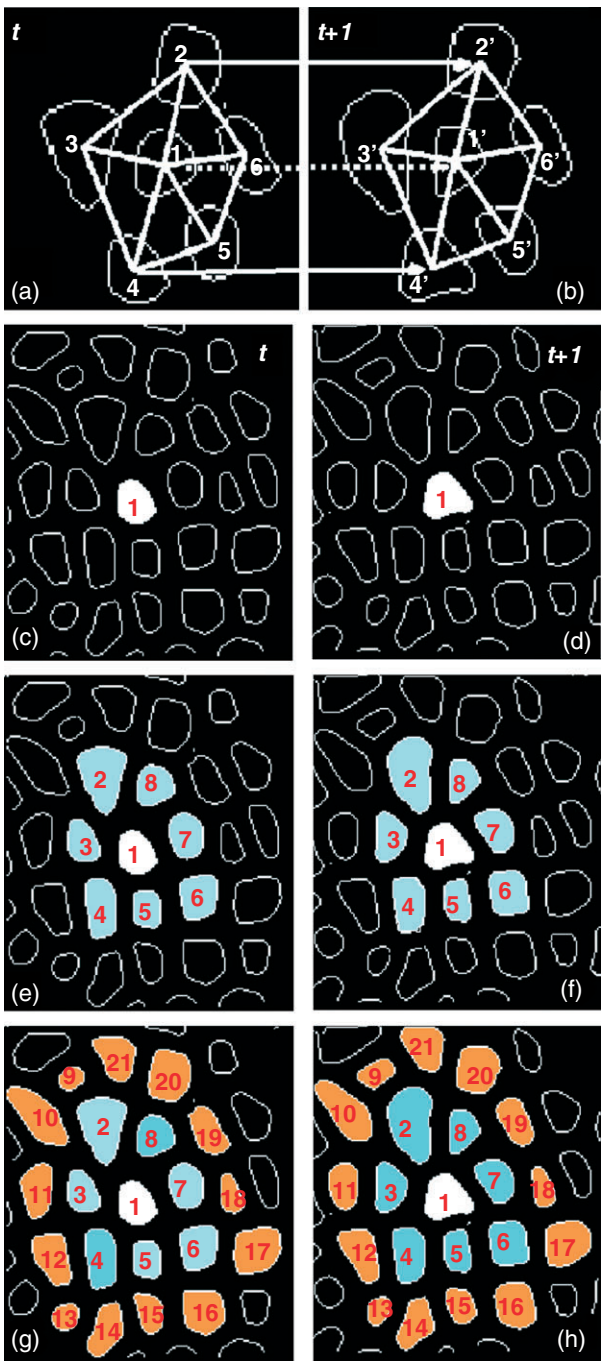

Figure 3. Growing correspondence from seed-pair.
(a, b) The matched local graphs G_1 at time instant t and G_2 at time instant $t + 1$, the correspondence of the seed cell pair (1, 1′), as well as the correspondences of the neighboring cells, such as (2, 2′) and (4, 4′). (c–h) The output from the procedure of growing correspondences among neighboring cells from a given seed pair (1, 1′).
(c, d) The seed cell pair.
(e, f) The tracking output after the first step of the recursion for growing the correspondences (the matched cells are numbered from 2 to 8).
(g, h) The tracking output after the second step of the recursion (the matched cell pairs are numbered 9–21). Note how the matching is progressing locally and radially outwards.

graphs with a similarity (distance) measure, as described in the following section.

Local graph matching

Given two local graphs G_1 and G_2 corresponding to cell c_i at time t and c_j at time $t + 1$, respectively (see Figure 3a,b), the distance measure $D_L(c_i, c_j)$ for these two graphs consists of three parts: the normalized difference of the edge lengths at consecutive time instants t and $t + 1$, the difference of the orientation angles between the edges, and normalized location difference information of cells. This distance measure can then be expressed mathematically as follows in equation 1:

$$D_L(c_i, c_j) = \frac{\lambda_1}{M} \cdot \sum_{c_m \in N(c_i),\, c_n \in N(c_j)} \frac{\left| l_{c_m, c_i}(t) - l_{c_n, c_j}(t+1) \right|}{l_{c_m, c_i}(t)} + \lambda_2 \cdot \frac{\left| A_{c_i}(t) - A_{c_j}(t+1) \right|}{A_{c_j}(t)} + \frac{\lambda_3}{M} \cdot \sum_{c_m \in N(c_i),\, c_n \in N(c_j)} \frac{\left| \theta_{c_m, c_i}(t) - \theta_{c_n, c_j}(t+1) \right|}{\theta_{c_m, c_j}(t)} + \lambda_4 \cdot \frac{\left\| \mathrm{P}_{c_i}(t) - \mathrm{P}_{c_j}(t+1) \right\|}{\Delta} (m = n = 1, \ldots, M),$$

where M is the number of neighboring cells in the two local graphs (they *must* be the same for the graphs to match), c_m is the mth neighboring cell of c_i, and c_n is the nth neighboring cell of c_j, $l_{c_m, c_i}(t)$ and $l_{c_n, c_j}(t+1)$ are the edge lengths, $\theta_{c_m, c_i}(t)$ and $\theta_{c_n, c_j}(t+1)$ are the orientation angles in radians of the edges measured relative to a horizontal axis, $A_{c_i}(t)$ and $A_{c_j}(t+1)$ are the size of the central cells' (c_i and c_j) area, $\mathrm{P}_{c_i}(t)$and $\mathrm{P}_{c_j}(t+1)$are the cell position vectors (here they are the central cells' coordinates in the registered image plane), and Δ is the average distance between two neighboring cells. The neighboring cells in the two graphs are ordered by orientation and distances are computed between the central cell and a neighboring cell having the same ordering number, i.e. $m = n = \{1,\ldots,M\}$. $|.|$ represents the magnitude of the difference between two scalars, while $\|.\|$ represents the Euclidean distance between two vectors. In practice, M can be set at a value lower than the total number of neighboring cells in order to account for segmentation errors.

If two local graphs match (i.e. the distance measure is small), the central cells (i.e. c_i and c_j) in those two local graphs are corresponding cells (a cell pair) (Figure 3a,b). This method was applied to two images (at two time instants or two slices at the same time instant) to identify the corresponding cells.

Finding the seed/initial cell(s) and recursive matching of neighboring cells

The above distance computation finds the similarity between two local graphs through the distance function based on the assumption that the topology of local graphs

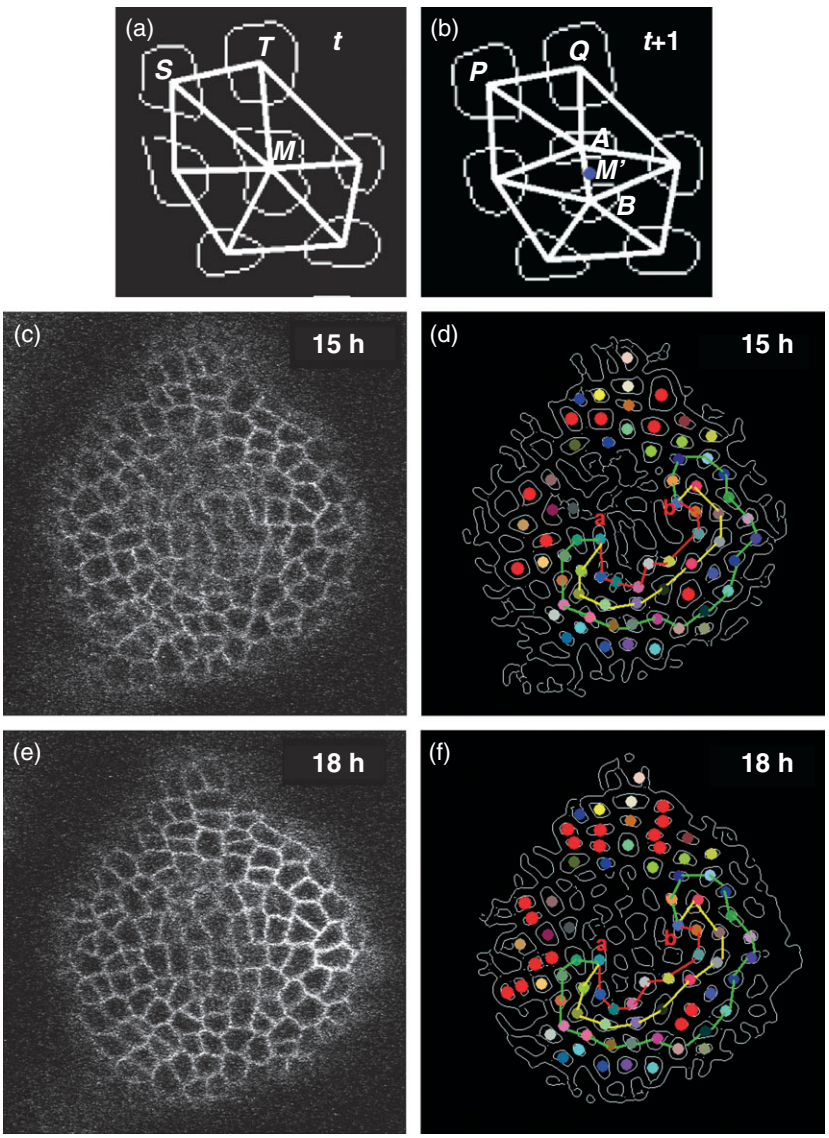

Figure 4. Detecting cell divisions and robustness of tracker by considering multiple correspondence paths.
(a, b) A conceptual description of the relative positions of a parent cell and its daughters. Here a parent cell *M, M'* at time point *t* divides into two sibling cells *A* and *B* at time point *t* + 1.
(d, f) represent tracking output including 8-cell division events, where the corresponding, non-dividing cells are denoted by the same color. For a dividing cell, the parent cells and corresponding sibling cells are denoted by red color. The three paths in red color, yellow color and green color demonstrate the feature of this algorithm that it can automatically grow cell correspondences from one pair to another pair by multiple paths. We show three such paths between cell 'a' and cell 'b' for two time points.
(c, e) Are the original image frames of (d, f) before segmentation.

does not change between two consecutive time instants and the changes in geometry of the local graphs are minimal. However, this fact may not always be true with SAM cells that show continuous growth and also every cell in the image field may not be imaged properly. Therefore, we devised a two part tracking strategy which involves finding the most similar cell pair as the seed pair, and then employing a slightly different distance measure to grow the matching process radially among the neighboring cells of the seed pair (see Equation 3 in supplementary section of Data S1 and Figure 3c–h). The main difference is that while the seed pair is computed from the neighborhood structure using local graph matching, tracks of other cells are found by computing the similarities along different paths of the graph (Reuille *et al.*, 2005). Mathematically, this means that in the seed computation (Equation 1) the distances are summed over the neighborhood, while in the Equation 3 of supplementary data, we only consider the distance between two neighbors without summation over the neighborhood set. This process ensures that as long as a single feasible path exists from the seed to the target cell, i.e. all cells in this path are imaged and segmented properly, we can compute the correspondences (Figure 3c–h).

As an example, Figure 4(d,f) show the tracking of cells across two consecutive time instants including seven cell division events (the corresponding cells are denoted by the same color). This example also demonstrates the robustness of the tracking method in finding the corresponding cell pairs despite noisy images, poor segmentation and also cell division events (Figure 4d,f). This robustness is attributable to the local graph matching method which has the capability to grow the correspondences to the neighborhood starting from a seed pair. In Figure 4, three such paths for growing the correspondences between two representative cells ('a'

and 'b') across two time instants have been shown which reveal that as long as the right seed pairs are chosen, the tracking algorithm will automatically identify a right path from the seed pair to any other cell pairs in the neighborhood. Therefore, even if some parts of the image are noisy, the correspondences among given cell pairs can be found with the availability of at least one feasible path (Figures S2, S3).

Detecting cell divisions

Based on the location, the cells of the SAMs divide at different rates (Grandjean *et al.*, 2004; Reddy *et al.*, 2004). It is expected that the topology of a given local graph will change upon cell division. Therefore, the changes in topology of local graphs act as good indicators of cell division events. Initial step in the process of cell division detection is finding the corresponding cell pair (M, A) across two time instants (t, $t + 1$) and it was accomplished through the correspondence growing procedure described in earlier section (Figure 3c–h). This was followed by examination of the differences in the areas of cells M and A (Figure 4). If the area difference of M and A is about half of the area of a parent cell, then we allow for the possibility that there maybe a cell division event resulting in two sibling cells. In this case, cell M may be the parent cell and cell A may be one of the daughter cells. If there is a cell division event, we should be able to find the other sibling cell among the neighboring cells of A. Specifically, we can search in the neighborhood around the original location M' of the parent cell at time $t + 1$ and the cell B with the shortest distance from M' should be the candidate for the other sibling cell. Furthermore, this distance should be within about half of the average distance between two neighboring undivided cells. Figure 4(a,b) illustrates this basic idea discussed above, where the parent cell is M and its two daughter cells are A and B.

In a more formal way, we are looking for the local graph structure (includes both topological and geometrical properties) to change in a particular way, as shown in Figure 4. This test for detecting possible cell division was carried out for each corresponding cell pair identified through the local graph matching process and it can automatically identify cell division events (Figure 4d,f). In order to evaluate the effectiveness of the cell tracking algorithm in identifying cell division events, the cell division events obtained from manual counting were compared with the events identified through the automatic method (Table 1). This analysis reveals that the local graph matching method can detect 100% of the cell divisions that are properly segmented and 96% in the unsegmented image data suggesting that the small percentage of error is due to the improper segmentation. A small fraction of over representation of cell division events has also been observed and these false positives that appear in the automatic method are due to the improper segmentation of cells (Table 1). Although our method is robust to some amount of noise in imaging and errors in segmentation, a consistently poor segmentation across all the slices and consecutive time instants may lead to poor performance, and we do need a reasonable quality of the data (the lowest signal-to-noise ratio in our experiment is 13.5 dB).

Table 1 Comparison of the number of cell division events between manual tracking (both in the unsegmented data and the segmented data, the latter being in parenthesis), and the automated method used in this study

Slice number in Z-stack	Time interval (h)	Number of cell divisions by manual detection	Number of cell divisions by automated method
Slice 2	0–30	14 (14)	14
Slice 3	0–39	21 (20)	20
Slice 4	0–42	34 (32)	32
Slice 5	0–57	48 (49)	49
Slice 6	0–63	55 (56)	56
Slice 7	0–72	55 (53)	53
Slice 8	30–72	38 (38)	38
Slice 9	30–72	54 (54)	54

The data for different slices are shown.

Fusion of spatial and temporal correspondence

The relative positions of SAM cells not only have temporal consistency, but they also have spatial consistency because every cell, in most cases, is represented in three consecutive optical slices (Figure 1a–i). This feature was exploited by the local graph matching method to find the spatial correspondence of cells across consecutive slices taken at different depths. Subsequently, the spatial and temporal correspondences were fused together to obtain a single unified track. This situation allowed us to track those cells that may have been poorly imaged in one slice, but are of a higher quality in a neighboring slice. In order to estimate the effectiveness of fusion of spatial and temporal tracks of cells in increasing the robustness of tracking, we compared the number of cells that are correctly tracked across two consecutive time instants with or without the fusion process (Table 2). The number of the cells obtained from manual counting both in the unsegmented image data and the automatically segmented data were used as ground truth to calculate the efficiency of the fusion process. The number of cells identified from three consecutive slices across two time instants from both the manual counting and automated tracking are also listed for comparison. This analysis reveals that fusion of the tracking output obtained from three independent consecutive slices of a given set of cells improves the tracking efficiency by increasing the robustness in obtaining temporal correspondence of cells (Table 2).

The shape of the SAM and the imaging method used for obtaining thin cross sections will result in sequential distri-

Table 2 Number of cells tracked manually (in the unsegmented data and in the segmented data) and automatically by the proposed tracking method (without the fusion process and with the fusion process)

Slice no. in Z-stack	Time interval (h)	Number of cells from manual tracking in unsegmented data	Number of cells from manual tracking in segmented data	Number of cells from automatic tracking without fusion	Number of cells from automatic tracking with fusion
Slice 4	3–6	87	68; 86; 85	63; 83; 80	86
Slice 4	6–9	86	85; 85; 91	83; 83; 80	84
Slice 5	18–21	102	99; 98; 94	94; 94; 86	95
Slice 5	21–24	75	81; 74; 80	75; 72; 77	74
Slice 7	3–6	100	96; 98; 105	89; 91; 94	95
Slice 7	6–9	122	113; 118; 116	103; 106; 94	115

For every slice, we also show the tracking results of the previous slice and that of the next slice before the fusion process.

bution of cells along different optical slices. Therefore obtaining correspondences among consecutive slices (Z-sections) will be crucial not only to introduce robustness to the tracking process but also to account for all cells of SAMs. However, maintaining the stability of tracks of cells located at different depths along the Z-axis of image stack can be challenging. Therefore, we tested the stability of tracks obtained for the topmost 12 slices of a Z-stack which account for all cells located within the CZ and the PZ of the L1 layer (Table 3). The comparison of tracking output for any two time instants with manual counting revealed that up to 95% of the correctly segmented cells could be tracked and up to 93% of cell division events could be detected (Table 3).

Computing cell lineages

The cell cycle lengths of cells located in distinct regions of SAMs vary from 18 to 90 h and plastochron length which reflects the time of initiation of successive organ primordia varies from 14 to 20 h (Callos *et al.*, 1994; Reddy *et al.*, 2004). Therefore understanding the cellular basis of morphogenesis requires tracking of cell lineages over longer periods of time. Computing cell lineages just by repeating the two-frame tracking process over the entire time series will result in a gradual loss of cells in the later time instants due to imaging noise, improper segmentation and tracking errors.

Table 3 Total numbers of cells and cell divisions tracked in the stack of the top 12 slices in different time intervals

Time interval (h)	Number of automatically tracked cells	Number of automatically tracked cell divisions
3–6	219/228	1/1
6–9	251/261	6/7
9–12	263/274	8/8
12–15	231/240	20/21
15–18	185/196	28/30

The denominator is the ground truth in the segmented data (the number of cells tracked manually or the number of cells divisions identified manually); the numerator is the tracking result obtained from the algorithm developed in this study.

In order to maintain the consistency of the cell lineages for long time periods, we have developed a method to integrate the tracks from multiple slices at a given time instant with that of tracks obtained across time periods. The idea here is that the lineage may be computed through multiple temporal paths (not to be confused with the spatial paths of Figure 4) as shown in Figure 8 and then fused together. Thus a cell that may not have been tracked along a particular path can still be part of final lineage computation if it was tracked in any of the other paths. Although this method introduces a delay in the system, this is not a major concern in this application domain as it will lead to higher accuracy in tracking and real-time performance is not necessary for this application domain (Figure 8 and discussed in detail in the methods section).

We have quantified the performance of our long-term cell-tracking algorithm in maintaining consistency of the cell lineages in time lapse series taken at 3-h intervals and extending up to a total of 72 h (Figure 7b). We considered cells located in the top eight slices of each image stack for this analysis. This analysis reveals that about 90% of the cells that were identified in the first time instant could be found 36 h later (Figure 7b). The sudden and a small decrease in the number of correctly tracked cells at 36 h is mostly due to the displacement of PZ cells into actively developing organ primordia (Figure 7b). We have also noticed that certain cells that were undetected from tracked output at 21 h could be recovered at 27 h indicating the usefulness of the method in long-term tracking (Figures 8 and 7b). The consistency of tracked output was maintained over 72 h despite repeated divisions of corresponding cells at different time intervals (Figures 5 and 7a). The frequency of cell division events at different time intervals reported by the tracker revealed temporal fluctuations in mitotic activity of SAM cells that is consistent with results obtained from manual tracking methods described earlier (Figure 7a) (Reddy *et al.*, 2004). Because cells are represented in more than one consecutive slice, there is a possibility that they may be tracked several times. In order avoid this redundancy in cell lineage estimation process, care was taken not to count a given cell

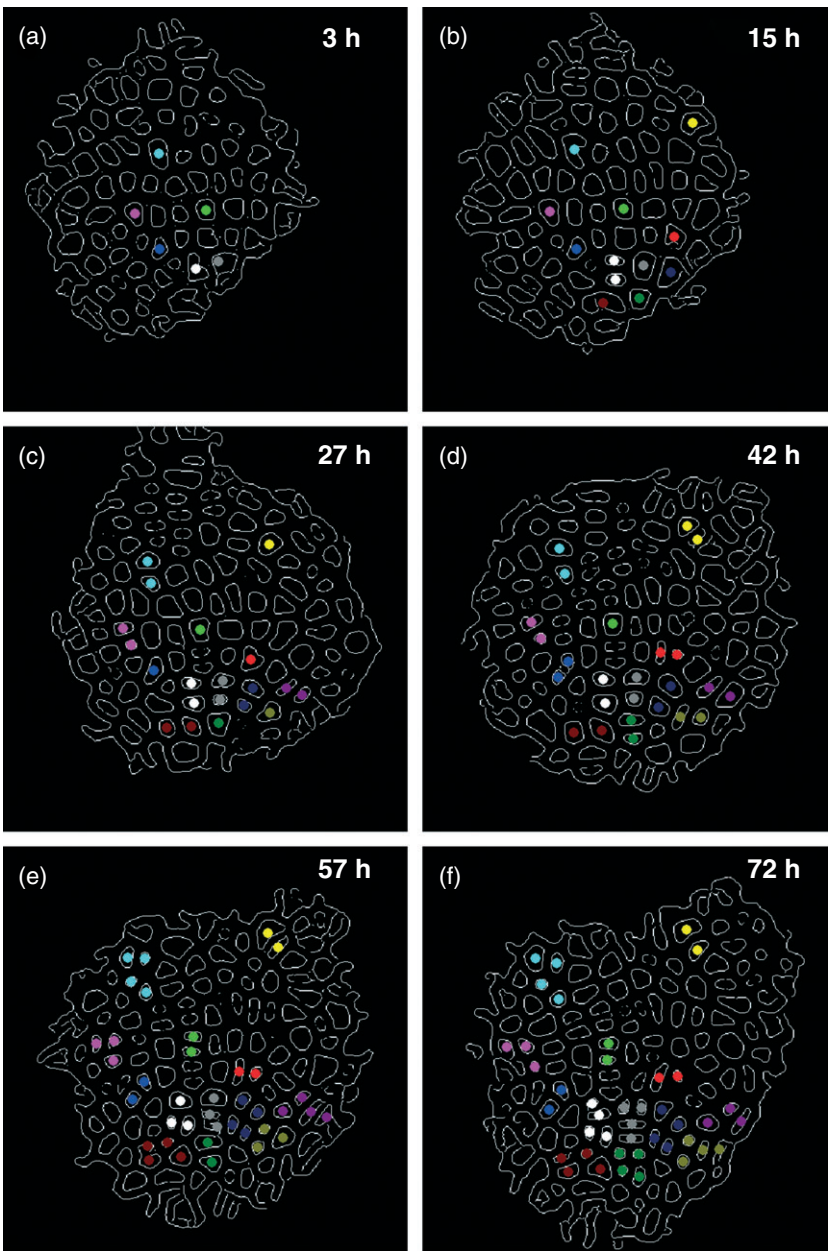

Figure 5. Computed cell lineages of SAM cells. (a–f) The cell lineages across 24 time instants (a total of 72 h of time-lapse data) were computed (only six frames are shown here, and only some cells' lineage are represented in this example), where the cell lineages are denoted by different colors. A complete version of the lineage in this example is shown in Figure S4. After 72 h of tracking, most of cells have divided at least once, while several of them divided twice or thrice.

more than once by finding correspondences of given cells in the pervious and the subsequent slices of the image stack. Similarly, when computing the final track for each cell, we provide only one track that was obtained from fusing the spatial and temporal correspondences.

Summary of the proposed algorithm for lineage computation

Input: A series of time-lapse images of Z-Stacks consisting of optical cross sections of SAMs (Figure 1).

Step 1: Segmentation of cells in Z-stacks using level-sets (Figures 3 and 4).

Step 2: Obtain correspondences of cells for a given slice between two time instants (this is done over a window of four consecutive time instants leading to six pairings). For every corresponding cell pair, check for cell division (refer to sections on local graph matching, recursive matching, and cell division detection).

Step 3: Obtain spatial correspondences of cells across slices of a given time instant (refer to Data S1, Correspondence across image slices).

Step 4: For every slice, fuse the spatial and temporal correspondences together for every two frames (six possible pairings) in the time window of four consecutive

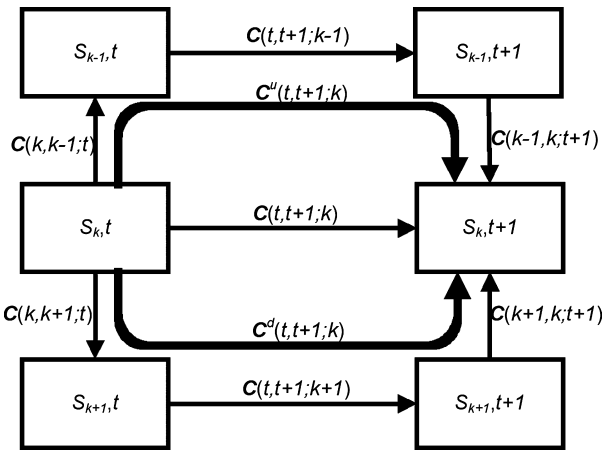

Figure 6. Diagrammatic representation of the process of fusion of the spatial and temporal correspondences of cells.
We consider three consecutive slices S_{k-1}, S_k and S_{k+1} to compute the final cell correspondence for slice S_k. As shown in Figure 1, every cell usually occupies three slices, so the integration of the tracking results from each one of the three consecutive slices improves the tracking performance. With this fusion process, we can obtain new cell pairs, which were not identified by single slice (S_k) tracking, but may be found through the tracking in the adjacent slices S_{k-1} or S_{k+1}.

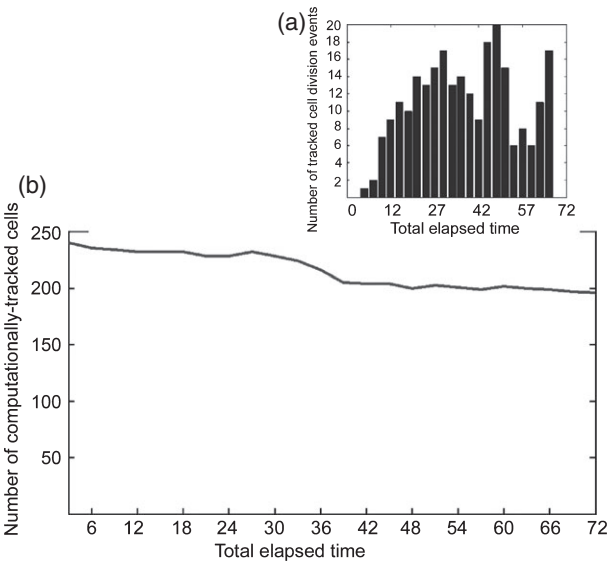

Figure 7. Stability of long-term tracking through multiple cell divisions.
(a) Total number of computationally-detected cell divisions in a time lapse series of 72 h (data from top eight slices have been integrated).
(b) Total number of computationally-tracked cells across different time instants measuring up to 72 h. Note the stability of tracking algorithm as most of the cells identified at first time instant could be detected at later time instants. The sudden decrease in the number of correctly tracked cells at 36 h is mostly due to the incorporation of cells located at the edge of the PZ and subsequent displacement of cells into actively growing organ primordia.

frames (refer to Data S1, Fusion of spatial and temporal correspondences, Figure 6 and Table 2).

Step 5: Compute final cell lineages by fusing the tracking results over the time window (refer Data S1, Final cell lineages computation).

Output: Lineages of all cells along all time instants (shown in Figures 5 and S4).

The code is available online at http://www.ee.ucr.edu/~amitrc/cell-dynamics.php.

DISCUSSION

In this paper, we have presented a local graph matching-based method to track cells and cell divisions from 4-D (3-D space + time) confocal microscopy images of SAMs. The main challenge in tracking cells of SAMs is that the cells that exist in clusters and they share very similar features. We have addressed this problem by exploiting the geometric structure and topology of the relative positions of cells. By matching the local graphs of related cells, we have computed spatio-temporal correspondences of both dividing and non-dividing cells. Finally we show that integration of outputs from spatial and temporal tracks increased the efficiency of the tracker in computing cell lineages over extended periods of time.

Our method is robust to imaging noise as it was able to maintain stability of the tracks which is a challenge in any visual tracking problem. The method requires input images to be approximately aligned, which can be achieved either by carefully placing the plant on the microscope platform or by using a suitable registration algorithm to globally align the images. The ability to maintain the stability of the tracks is also dependent on the imaging interval. If the imaging intervals are too long, the multiple divisions within a neighborhood between two consecutive time-lapse images can change the neighborhood topology significantly that makes it difficult to compute similarities.

Pattern formation in SAMs requires precise spatio-temporal coordination of cell growth and cell division patterns with that of gene expression patterns, mediated by cell–cell communication networks. The distinct spatial domains of gene expression of SAMs are maintained despite the continuous flux of cells from undifferentiated stem-cells into differentiating organs. The molecular mechanisms regulating the process of stem-cell maintenance and also the process by which regular arrangement of lateral organs is achieved in well understood. The gene expression and growth dynamics underlying these processes are beginning to be unraveled mainly due to the development of live-imaging methods (Grandjean *et al.*, 2004; Heisler *et al.*, 2005; Reddy and Meyerowitz, 2005; Reddy *et al.*, 2004). However, quantitative description of the relationship between cell expansion and cell division orientation, and the causal relationship between cell division patterns and the gene expression patterns, have not been understood. Moreover, a quantitative determination of the spatiotemporal parameters of signaling components of cell–cell commu-

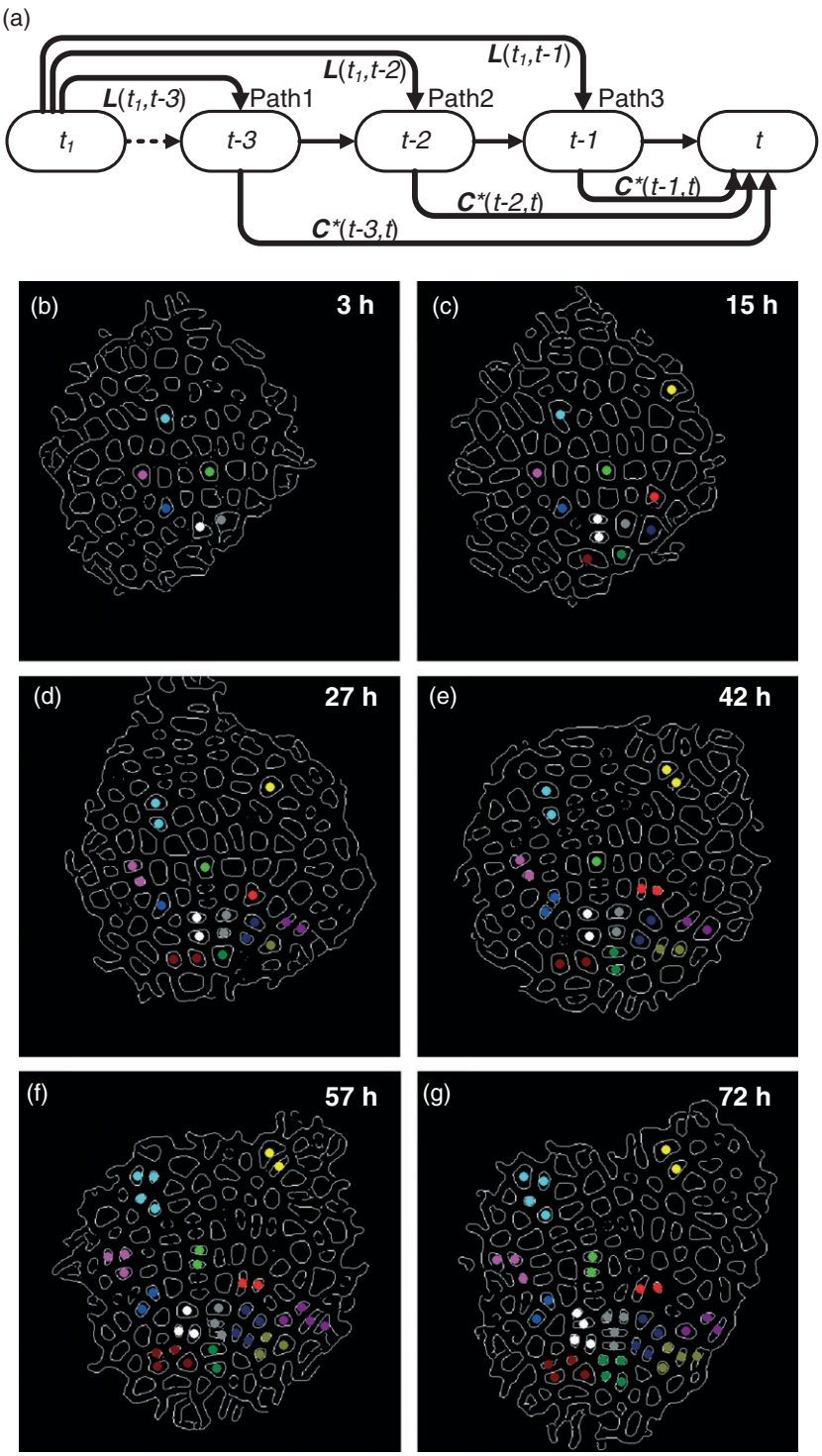

Figure 8. Final cell lineage computation.
(a) Cell lineage (from time t_1 to t) computation process by fusing along multiple tracking paths (Path 1, Path 2 and Path 3).
(b, c) Cell lineages from time 6 to 18 h, computed by Path 1.
(d, e) Cell lineages computed by Path 2.
(f, g) Cell lineages computed by the combination of Path 1 and Path 2. Note that the system may lose correspondence of some cells along a particular path, but maintained their correspondences in an alternate tracking path. Compare (b), (d) and (f), cells in green circles were lost in (b) and (c) while cells in red circles were lost in (d) and (e), but all of them were gained back in (f) and (g) due to the fusion process.

nication networks can be challenging considering the complex topology of SAM surface and limited intracellular-spatial resolution because of the smaller cell size. However, most of our quantitative understanding of SAM growth comes from studies either derived from tedious manual analysis of live-imaging data or from the reconstructed replicas of SAMs (Dumais and Kwiatkowska, 2002; Kwiatkowska and Dumais, 2003; Reddy *et al.*, 2004; Kwiatkowska, 2006; Szczesny *et al.*, 2009). Therefore, a quantitative understanding of pattern formation process requires development of computational models of cell growth and cell division. While there is significant work in tracking cells in video, most of the methods concentrate on tracking in 2-D. However, a major task in quantifying gene

expression dynamics is to estimate the dynamics of 3-D cell volumes, which would require tracking in 3-D. The main challenges in 3-D tracking are: (i) developing a robust method for extracting/isolating 3-D cells across layers; (ii) representing the cell shape using a suitable shape descriptor; (iii) 3-D tracking methods that are able to maintain the correlations across the layers, as well as in time; and (iv) learning deformation models to describe cell shape changes which can then be used for volume estimation. The new cell tracking method introduced in this study should allow us to quantify the 3-D cell growth dynamics over longer periods of time and this can be combined in the future with gene expression dynamics to understand the mutual regulation with an ultimate aim of developing dynamic developmental atlas of SAMs.

A major challenge, however, in developing a dynamic gene expression atlas is to transform static transcriptome maps into dynamic spatial-temporal maps (atlas), representing gene expression dynamics on realistic cellular templates (Yadav *et al.*, 2009). The live-imaging studies have revealed variability in size and shapes of SAMs, and also total number of cells/SAM within a population of *Arabidopsis* plants. Given the fact that it is not possible to label and visualize more than a few (may be up to 3 or 4/SAM) genes or proteins in a single SAM, it is necessary to develop computational platforms which will facilitate comparisons of corresponding gene expression domains from different SAMs with differing sizes and shapes. Therefore, new computational thinking is required; first, to map corresponding regions/gene expression patterns from several different SAMs into a single composite template, and second, to obtain temporal correspondences between different SAMs. The primary step in addressing this issue is to learn the mathematical models that can capture the similarities and variations in the growth patterns of cells and expression patterns of corresponding genes across different SAMs through recognition and spatio-temporal modeling of inherent dynamical patterns. The image analysis tools, introduced in this study, for obtaining cell segmentation, detecting cell divisions and tools for long-term tracking of cell lineages would facilitate both learning dynamical models of growth and modeling the variations in the growth patterns across SAMs.

EXPERIMENTAL PROCEDURES

Transgenic lines, growth conditions and live-imaging

The development of stable transgenic plants ubiquitously expressing a plasma membrane marker (35S::29–1 YFP) have been described earlier (Reddy *et al.*, 2004). All plants grown either on soil or on plates are maintained in continuous light and at 20–22°C. For live imaging, plants were grown on MS-agar plates for 10 days before they were transferred into the clear plastic boxes containing MS-agar. Upon bolting, the plants were prepared for time-lapse imaging by removing the older floral buds to expose the shoot apical meristem surface and by stabilizing the rosette by applying 1.5% molten agarose onto the stem. Plants were imaged on Zeiss510 up-right confocal microscope by using a × 63 water dipping achroplan lens with an argon laser at 515 nm. The confocal Z-stacks of 1.5 μm step size were collected across time points and they were aligned by using an image registration software, MIRIT (Maes *et al.*, 1997). The registered four-dimensional Z-stacks were used in subsequent analysis described below.

Selection of computational parameters

All measurements here are represented in the image plane. Based on the confocal imaging geometry, these can be translated to the real-world measurements and adapted for a different imaging set-up. We make an assumption here that two cells across two time instants are considered corresponding cells if these conditions are satisfied: the normalized difference in length of the edge is less than 0.1, the orientation difference of the same edge is within 0.17 radians (10°) the normalized difference of cells' location is within 0.2, and the normalized difference of cell area is within 0.2. So in order to normalize the distance measures for different physical parameters, we set $\lambda_1 = 2$ and $\lambda_2 = \lambda_3 = \lambda_4 = 1$ and then the typical threshold for D_L and D_S would be 0.8 while D_N would be 0.6. Since all the distances are normalized, we do not need to translate them to the real-world values. Here, in different cases we can set different weights. Generally, in the well registered image data, we can set a bigger weight to λ_4 for the normalized difference of cells' location, while in those data that are not well registered, we can set bigger weights to λ_1, λ_2 and λ_3, because the associated differences are translation invariant. If there are no rotation and scaling effects in the imaging process, we can just discard the location difference (i.e. $\lambda_4 = 0$), without any appreciable decrease in performance. Moreover, if the normalized area difference of a corresponding cell pair is beyond 0.5, it was considered that there may be a cell division event. For a cell division event, the distance between the two daughter cells should be half of the average distance between two neighboring parent cells.

ACKNOWLEDGEMENTS

We thank the microscopy core facility of the Center for Plant Cell Biology (CEPCEB), and the Institute of Integrative Genome Biology (IIGB), University of California, Riverside. This work is funded by National Science Foundation grants [(IIS-0712253) to ARC and (IOS-0718046) to GVR].

SUPPORTING INFORMATION

Additional Supporting Information may be found in the online version of this article:

Figure S1. Segmentation of SAM cells.

Figure S2. Tracking output (right panel) showing 2-cell division events (shown in red color) on a data set from second SAM.

Figure S3. Tracking output (b and d) on a noisy confocal cross sections of SAMs (a and c) (some cells within the red circle are not imaged properly).

Figure S4. A complete time series showing consistency in cell tracking.

Figure S5. Cell lineage tree. The cell lineages along four time instants are denoted for different cells denoted by color-coded lines. Every cell has been denoted with a number and the divided daughter cells are denoted by the same number.

Figure S6. Representation of a 3-D cell lineage tree.

Figure S7. Cell growth dynamics of representative examples of three cells prior to and after cell division events.

Figure S8. A histogram showing variation in cell size of parent cells at the time of cell division.

Figure S9. Performance of cell tracker in high curvature regions.

Figure S10. Tracking output for cells of the L2 layer denoted by yellow circles.
Figure S11. Cell tracking results for time interval of 9 and 12 h.
Data S1. Experimental procedures.
Please note: As a service to our authors and readers, this journal provides supporting information supplied by the authors. Such materials are peer-reviewed and may be re-organized for online delivery, but are not copy-edited or typeset. Technical support issues arising from supporting information (other than missing files) should be addressed to the authors.

REFERENCES

Callos, J.D., DiRado, M., Xu, B., Behringer, F.J., Link, B.M. and Medford, J.I. (1994) The forever young gene encodes an oxidoreductase required for proper development of the *Arabidopsis* vegetative shoot apex. *Plant J.* **6**, 835–847.

Chan, T. and Vese, L. (2001) Active contours without edges. *IEEE Trans. Image Process.* **10**, 266–277.

Chui, H. (2000) A new algorithm for non-rigid point matching. *IEEE Comput. Soc. Conf. Comput. Vis. Pattern Recognit.* **2**, 44–51.

Cutler, S.R., Ehrhardt, D.W., Griffitts, J.S. and Somerville, C.R. (2000) Random GFP::cDNA fusions enable visualization of subcellular structures in cells of *Arabidopsis* at a high frequency. *Proc. Natl Acad. Sci. USA*, **97**, 3718–3723.

Dumais, J. and Kwiatkowska, D. (2002) Analysis of surface growth in shoot apices. *Plant J.* **31**(2), 229–241.

Fazl-Ersi, E., Zelek, J.S. and Tsotsos, J.K. (2007) Robust face recognition through local graph matching. *J. Multimed.* **2**, 31–37.

Gold, S. and Rangarajan, A. (1996) A graduated assignment algorithm for graph matching. *IEEE Trans. Pattern Anal. Mach. Intell.* **18**, 377–388.

Gor, V., Elowitz, M., Bacarian, T. and Mjolsness, E. (2005) Tracking cell signals in fluorescent images. *IEEE Workshop on Computer Vision Methods for Bioinformatics*, pp. 142–150.

Grandjean, O., Vernoux, T., Laufs, P., Belcram, K., Mizukami, Y. and Traas, J. (2004) In vivo analysis of cell division, cell growth, and differentiation at the shoot apical meristem in *Arabidopsis*. *Plant Cell*, **16**, 74–87.

Heisler, M.G., Ohno, C., Das, P., Sieber, P., Reddy, G.V., Long, J.A. and Meyerowitz, E.M. (2005) Auxin transport dynamics and gene expression patterns during primordium development in the *Arabidopsis* inflorescence meristem. *Curr. Biol.* **15**, 1899–1911.

Hernandez, L.F., Havelange, A., Bernier, G. and Green, P.B. (1991) Growth behavior of single epidermal cells during flower formation: sequential scanning electron micrographs provide kinematic patterns for *Anagallis*. *Planta*, **185**, 139–147.

Kwiatkowska, D. (2004) Surface growth at the reproductive shoot apex of *Arabidopsis thaliana* pin-formed 1 and wild type. *J. Exp. Bot.* **55**, 1021–1032.

Kwiatkowska, D. (2006) Flower primordium formation at the *Arabidopsis* shoot apex: quantitative analysis of surface geometry and growth. *J. Exp. Bot.* **57**, 571–580.

Kwiatkowska, D. and Dumais, J. (2003) Growth and morphogenesis at the vegetative shoot apex of Anagallis arvensis L. *J. Exp. Bot.* **54**, 1585–1595.

Laufs, P., Grandjean, O., Jonak, C., Kieu, K. and Traas, J. (1998) Cellular parameters of the shoot apical meristem in *Arabidopsis*. *Plant Cell*, **10**, 1375–1390.

Li, K. and Kanade, T. (2007) Cell population tracking and lineage construction using multiple-model dynamics filters and spatiotemporal optimization. *Second International Workshop on Microscopic Image Analysis with Applications in Biology*. September 21.

Lyndon, R.F. (1998) *The Shoot Apical Meristem: Its Growth and Development*. Cambridge: Cambridge University Press.

Maes, F., Collignon, A., Vandermeulen, D., Marchal, G. and Suetens, P. (1997) Multimodality image registration by maximization of mutual information. *IEEE Trans. Med. Imaging*, **16**, 187–198.

Meyerowitz, E.M. (1997) Genetic control of cell division patterns in developing plants. *Cell*, **88**, 299–308.

Rangarajan, A., Chui, H. and Bookstein, F.L. (2005) The Softassign procrustes matching algorithm. In: *Information Processing in Medical Imaging*. New York: Springer, pp. 29–42.

Reddy, G.V. and Meyerowitz, E.M. (2005) Stem-cell homeostasis and growth dynamics can be uncoupled in the *Arabidopsis* shoot apex. *Science*, **310**, 663–667.

Reddy, G.V., Heisler, M.G., Ehrhardt, D.W. and Meyerowitz, E.M. (2004) Real-time lineage analysis reveals oriented cell divisions associated with morphogenesis at the shoot apex of *Arabidopsis thaliana*. *Development*, **131**, 4225–4237.

Reuille, P.B., Bohn-Courseau, I., Godin, C. and Traas, J. (2005) A protocol to analyse cellular dynamics during plant development. *Plant J.* **44**, 1045–1053.

Steeves, T.A. and Sussex, I.M. (1989) *Patterns in Plant Development: Shoot Apical Meristem Mutants of Arabidopsis thaliana*. New York: Cambridge University Press.

Szczesny, T., Routier-Kierzkowska, A.-L. and Kwiatkowska, D. (2009) Influence of clavata3–2 mutation on early flower development in *Arabidopsis thaliana*: quantitative analysis of changing geometry. *J. Exp. Bot.* **60**, 679–695.

Viola, P. and Wells, M.W. III (1995) Alignment by maximization of mutual information. *Fifth International Conference on Computer Vision*, pp. 16–23.

Yadev, R.K., Girke, T., Pasala, S., Xie, M.T. and Reddy, G.V. (2009) Gene expression map of the Arabidopsis shoot apical meristem stem cell niche. *Proc. Natl. Acad. Sci.* **106**, 4941–4945.

Zheng, Y. and Doermann, D. (2006) Robust point matching for nonrigid shapes by preserving local neighborhood structures. *IEEE Trans. Pattern Anal. Mach. Intell.* **28**, 643.

